Chemical and Electrochemical Intercalation of Lithium in 2D-$FeMoO_4Cl$[1]

Jin-Ho Choy*, Soon-Ho Chang†, Dong-Youn Noh, and Kyoung-A Son

Department of Chemistry, Seoul National University, Seoul 151-742

†Laboratoire de Chimie du Solide du C.N.R.S. Talence Cedex 33405, France. *Received July 15, 1988*

Lithium has been intercalated into $FeMoO_4Cl$, and deintercalated from Li_xFeMoO_4Cl both electrochemically and chemically. The inserted Li^+ ions are stabilized in the distorted octahedral field in interlayer space of $FeMoO_4Cl$. The crystal symmetry is reduced from tetragonal to monoclinic due to the reduction of ferric to ferrous ions in Li_xFeMoO_4Cl upon lithium intercalation. From the magnetic and structural data, it has been concluded that the high-spin electronic configuration of $Fe^{2+}(d_{xz}^2 d_{yz}^1 d_{xy}^1 d_{z^2}^1 d_{x^2-y^2}^1)$, corresponding to ^5E_g group term in D_{4h} symmetry, can be stabilized by the elongation of FeO_4Cl_2-octahedra in a weak ligand field.

Introduction

$FeMoO_4Cl$ is a layer compound which has the tetragonal symmetry with unit cell parameters $a = 6.672$ Å and $c = 5.223$ Å, space group P4/nmm and $Z = 2$. The individual $FeMoO_4Cl$ layers are extended two-dimensionally by corner-sharing between slightly distorted tetrahedral MoO_4 with site symmetry of $\bar{4}2m$ (D_{2d}) and square pyramidal FeO_4Cl with that of 4mm (C_{4v}) as shown in Figure 1-a. From atomic position in the $FeMoO_4Cl$-unit cell, the lattice can be described as two layers of chlorine ions sandwiched by corrugated metal-oxygen plane. Due to the open nets of chlorine atom in the basal plane, adjacent layers interpenetrate each other and consequently each chlorine atom dips into the cavity formed by four oxygen atoms of basal FeO_4Cl in a neighboring layer. Because of this structural peculiarity, the chemical bonding between the sheets may be considered to be not only by van der Waals force, but also by weak covalent bonding.

Comparing the bonding character between individual sheets of $FeMoO_4Cl$ and those of FeOCl (van der Waals type only), one can explain with ease why $FeMoO_4Cl$ lattice could be less easily expanded by molecular intercalation than FeOCl one. It is why no molecular intercalation complexes have been so far characterized unequivocally, except the formation of alkali metal intercalation compounds. At present moment, it is therefore impossible to predict that a certain guest species could be intercalated into the interlayer space of $FeMoO_4Cl$. But from our previous experiences on the preparation of FeOCl intercalation complexes, we could find, for the first time, that lithium can intercalate into $FeMoO_4Cl$ lattice not only chemically but also electrochemically.[2]

The present paper deals with the synthesis of Li_xFeMoO_4Cl intercalates ($x = 0$, 0.20, 0.40, and 0.92) and the effect of lattice disorder and nonstoichiometry on the intercalation properties of $FeMoO_4Cl$ after electrochemical lithiation.

Experimental

(A) Preparation

$FeMoO_4Cl$ single crystals have been prepared by heating a mixture, the chemical vapor transport (CVT) technique, of Fe_2O_3, MoO_3, and $FeCl_3$ with a molar ratio of 1:3:1.05 in a vacuum sealed pyrex ampoule at the temperature gradient of 400-450 °C for several days. The product was washed with absolute ethanol repeatedly to remove the excess ferric chloride, and then dried under vacuum.

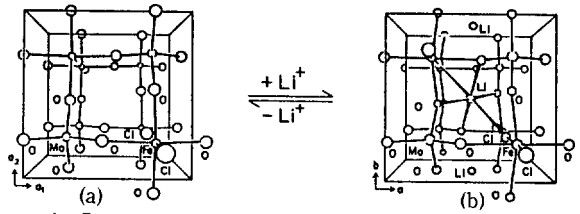

Figure 1. Reversible transition between (a) 2D-tetragonal (a = 6.672, b = 5.223 Å) and (b) 3D-monoclinic structure (a = 7.031, b = 6.910, c = 5.040 Å β = 91.30°)[6] upon lithium intercalation.

Chemical lithiation was carried out with lithium iodide in dried acetonitrile at ambient temperature for a week under an argon atmosphere. Lithiation of $FeMoO_4Cl$ led to a gradual color change from brown to black over several hours. After intercalation reaction, the lithiated product was carefully washed with dried acetonitrile and kept in vacuum.

Electrochemical study was carried out with a two-electrode cell of the form:

$$\text{Anode(Li)/(Li}^+, \text{ClO}_4^-) + \text{P.C./Cathode(FeMoO}_4\text{Cl)}$$

The cathode consists of finely ground $FeMoO_4Cl$ of about 90 mg mixed with graphite (up to 30% by weight) in order to enhance the electronic conductivity at macroscopic scale. Lithium perchlorate solution (1M) in propylene carbonate absorbed in glass-wool disc was used as the liquid electrolyte. Cells were galvanostatically charged and discharged at constant current densities of 30-50 $\mu A/cm^2$ under an argon atmosphere for a few days. Electrochemical processes at electrodes during charge-discharge cycle, can be described as follows:

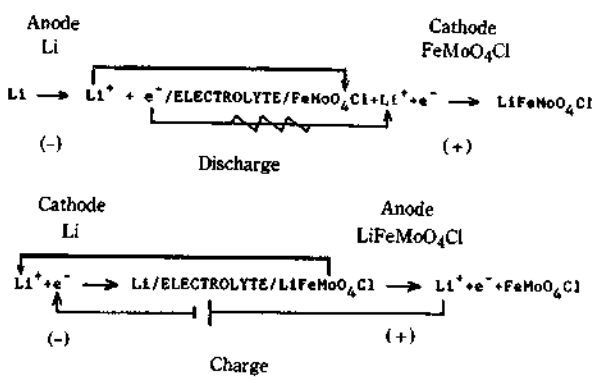

Figure 2. Scanning Electron Micrograph (SEM) of $FeMoO_4Cl$ single crystals with plate-like morphology (×5000).

Figure 3. Scanning Electron Micrograph (SEM) of $FeMoO_4Cl$ single crystals with board-like morphology (×5000). Typical edges of stacked $FeMoO_4Cl$-layers are clearly shown.

The electrode materials recovered at different intercalation degrees have been washed with absolute hexane, dried under vacuum and used for X-ray diffraction and spectroscopic analyses.

(B) Analysis

The microstructure images of $FeMoO_4Cl$ crystals were obtained by Scanning Electron Microscope (SEM), JEOL.

Iron and molybdenum contents were determined by a PERKIN-ELMER #4000 atomic absorption spectrophotometer with appropriate hollow cathode tube. Chlorine content was determined by the modified Volhard method.[3]

X-ray powder diffraction patterns were obtained either by the Debye-Scherre method in sealed capillaries or by a JEOL JDX-5P diffractometer with Ni-filtered Cu-K_α radiation (λ = 1.5418 Å). NaCl powder (a = 5.639 Å) was used as internal standard.

The EPR measurement was carried out on a BRUKER ER 200tt X-band spectrometer (9.75 GHz) at ambient temperature.

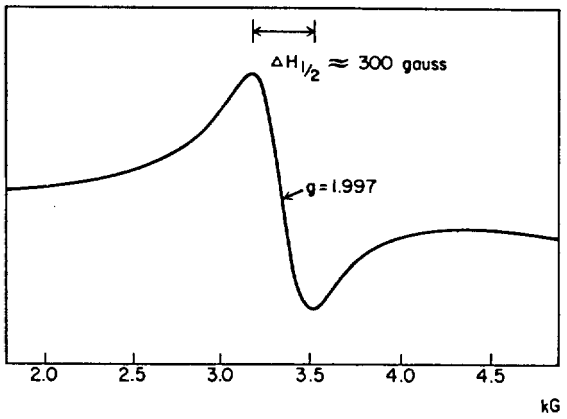

Figure 4. X-band EPR spectrum of $FeMoO_4Cl$ at ambient temperature.

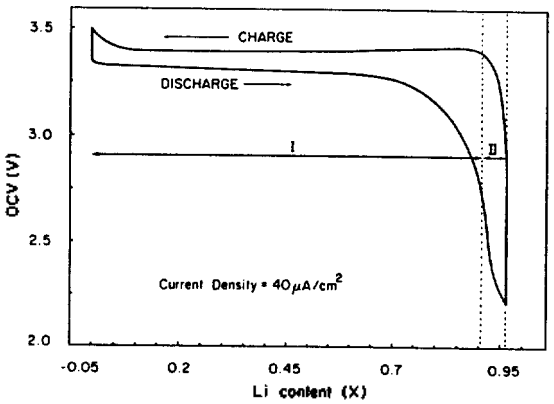

Figure 5. Open circuit voltage (V) vs intercalated Li content (x) in a Li// $FeMoO_4Cl$ cell. Two different regions of biphase domain(I) and solid solution domain(II) are denoted.

Results and Discussion

$FeMoO_4Cl$ single crystal could be grown up to ~10 mm in size by CVT technique. Its color in bulk is dark-red, but turns out to red-yellow after fine grinding. According to the SEM observation, the well-grown $FeMoO_4Cl$ crystals could be identified as a layer-type (Figure 2) or board-like (Figure 3) morphology. Especially their typical edges could be easily observed by oriented mounting technique as shown in Figure 3. The face of board-like sheet is a_1a_2-plane of tetragonal structure, to which c-axis is perpendicular. Two-dimensional $FeMoO_4Cl$ sheets are stacked in regular sequence along the c-axis to form layered structure. X-ray powder diffraction analysis indicates that $FeMoO_4Cl$ has tetragonal symmetry with lattice parameters of a = 6.668 and c = 5.231 Å which are consistent with previous report.[4] Stoichiometry of the title compound was also determined by chemical analyses in weight percent as follows: Calculated: Fe(23.3), Mo(38.2), Cl(14.1). Found: Fe(22.6), Mo(38.5), Cl(13.9).

Table 1. Observed d-Values (Å) for Tetragonal (Tg) and Monoclinic (Mono) Cells in $Li_xFe^{3+}_{1-x}Fe^{2+}_xMoO_4Cl$ ($0 \leq x < 1$)

(hkl) \ X	0		0.20		0.40[1]	0.92[1,2]
Tg	Mono	Tg	Tg	Mono	Mono	Mono
	100					7.109
001		5.231	5.262			
	001			5.068	5.068	5.068
	-101			4.138		4.157
101		4.114				
	(011 / 101)					4.086
	-111			3.569	3.569	3.569
	200			3.524	3.524	3.524
111		3.506				
	020			3.466	3.466	3.466
200		3.339	3.348			
	-201			2.928	2.928	2.928
	(021 / 201)			2.858	2.858	2.867
201		2.818	2.823			
	220			2.471	2.471	2.471
	012			2.365	2.365	2.365
220		2.350				
112		2.287	2.294			
	-112			2.261	2.261	2.261
	(112 / -221)			2.235	2.235	2.235
	221			2.206	2.206	2.206
	301					2.115
	031					2.101
	-311			2.051	2.051	2.051
301		2.032				
	(-131 / 311)					2.021
	131					2.007
311						
131		1.959	1.960			
	400			1.762	1.763	1.763
	040			1.732	1.732	1.732
	-312					1.688
400		1.667	1.671			
	-132					1.660
(312 / 132)		1.645				

[1]Graphite was mixed with the samples to improve the conductivity.
[2]$a = 6.99$ $b = 6.87$ $c = 5.01$ Å $\beta = 91.3°$.

From the EPR measurement, a broad singlet spectrum was observed at $g = 1.997$, its line shape being almost Lorentzian (Figure 4). It is well known that ferric ion with an axial C_{4v} symmetry resonates at $g_{eff} = 2.0$,[5] and molybdenum (VI) has no unpaired electron and does not contribute to the paramagnetism of the compound. Therefore the signal with $g = 1.997$ is surely from the paramagnetic ferric ions stabilized in C_{4v} field of oxychloride lattice.

Lithium complexes $Li_xFe^{3+}_{1-x}Fe^{2+}_xMoO_4Cl$ with different intercalation degrees of $x = 0.20$, 0.40, and 0.92 could be obtained by cathodic reduction of $FeMoO_4Cl$. Open circuit voltage (OCV) vs lithium content (x) gives a typical curve with an excellent reversibility over the compositional range $0 \leq x < 1$ (Figure 5). The x-ray diffraction patterns of the electrode materials recovered at four different steps are listed in Table 1. Comparing the reduction potentials of ferric ion (0.67 V in 0.5 M H_2SO_4) and molybdenum (VI) (0.40 V in 0.5 M H_2SO_4), it is obvious that the intercalated lithium ions reduce ferric to ferrous ion preferentially rather than molybdenum (VI). Lithium ions intercalated in the distorted octahedral sites between 2-dimensional layers, as shown in Figure 1-b, connect neighboring sheets. It is interesting to note that the lithium intercalates of $Li_{0.2}FeMoO_4Cl$ and $Li_{0.4}FeMoO_4Cl$ could not form a solid solution, rather to form biphase with the mixture of monoclinic $LiFeMoO_4Cl$ and unreacted tetragonal $FeMoO_4Cl$. The gradual transition from tetragonal to monoclinic phase is observed as the increase of lithium content(x). Due to the lithium intercalation and the expansion of electron density in d-orbitals upon reduction ($Fe^{2+} \leftarrow Fe^{3+}$), the gradual transition of crystal symmetry from tetragonal to monoclinic could be observed along with the change in structural dimensionallity (2D → 3D). The crystallinity of $Li_{1+x}FeMoO_4Cl$ has been strongly reduced and become amorphous by successive electrochemical lithiation, which might be due to the reduction of molybdenum (VI) to (V).

The effective magnetic moment of 5.67 BM (Cm = 4.02 emu/mole) and the Weiss constant of −204 K could be estimated from the magnetic susceptibility measurement of $Li_{0.92}FeMoO_4Cl$. The difference of magnetic moment between unlithiated (6.46 BM) and lithiated Fe(III)MoO_4Cl is 0.79 BM, which is consistent with the difference of spin number of Fe by formation of $Li_{0.92}FeMoO_4Cl$. From magnetic and structural analyses, it has been understood that the local symmetry of iron has been changed from C_{4v} (Fe(III) in Fe(III)MoO_4Cl) to D_{4h} (Fe(II) in $Li_{0.92}$Fe(II)MoO_4Cl). A high-spin state of Fe(II) with $t_{2g}^4e_g^2$ in Oh symmetry can be characterized by $^5T_{2g}$ term ($S = 2$). The Dq/B value for the spin crossover can be determined from a Tanabe-Sugano diagram[7] established for d^6 ion:

$$^5T_{2g} \longleftrightarrow {}^1A_{1g} \qquad Dq/B = 2.0$$

With a tetragonal distortion leading to $D_{4h} \leftarrow$ Oh, the ground term of $^5T_{2g}$ will be splitted to ^5E_g term with an electronic configuration of $e_g^3b_{2g}^1a_{1g}^1b_{1g}^1(d_{xz}^2d_{yz}^1d_{xy}^1d_{z^2}^1d_{x^2-y^2}^1)$. Hence the structural analysis, the magnetic susceptibility measurement, and the discussion of the local symmetry indicate obviously that the high-spin configuration of ^5E_g can be stabilized by a strong elongation of FeO_4Cl_2-octahedral in a weak crystal field of $Dq/B < 2$.

Acknowledgement. A part of this work was carried out with the S. N. U. Daewoo Research Fund in 1987.

References

1. This is the 2nd contribution after the 1st paper reported in *Mat. Res. Bull.* **23**, 73 (1988), of which the acknowledgement should also refer to S. N. U. Dae woo Research Fund.
2. J. H. Choy, D. Y. Noh, J. C. Park, S. H. Chang, C. Delmas, and P. Hagenmuller, *Mat. Res. Bull.*, **23**, 73

(1988).
3. L. Meites, "Handbook of Analytical Chemistry", 1st ed. McGraw Hill Co., Inc. (1963).
4. C. C. Torardi, J. C. Calabrese, K. Lázár, and W. M. Reiff, *J. Solid State Chem.*, **51**, 376 (1984).
5. G. E. Pake, and T. L. Estle, "The Physical Principles of Electron Paramagnetic Resonance" 2nd ed., W. A. Benjamin, Inc. (1973).
6. C. C. Torardi, W. M. Reiff, K. Lázár, and E. Prince, *J. Phys. Chem. Solids*, **47**, 741 (1986).
7. Y. Tanabe, and S. Sugano, *J. Phys. Soc. Jpn.*, **753**, 766 (1954).

A Study on the Characterization on Some Semiconductor Materials by Neutron Activation Analysis. Characterization of Semiconductor Silicon

Chul Lee*, Oh Cheun Kwun, Ho Kun Kim, Jong Du Lee†, and Koo Soon Chung‡

Department of Chemistry, Hanyang University, Seoul 133-791
†Korean Advanced Energy Research Institute, Seoul 139-240
‡Department of Chemistry, Sogang University, Seoul 121-742. *Received July 22, 1988*

Traces of nine elements, gold, arsenic, cobalt, chromium, copper, europium, hafnium, sodium and antimony in commercially available silicon crystals were determined by the instrumental neutron activation analysis using the single comparator method. The values of the concentrations of these elements in both single and polycrystals were found to decrease significantly to a low limiting level by simply washing and etching surface contaminants having been introduced during various steps of sample preparation and irradiation. However, the chromium levels in polycrystals were not easily decreased, these depending upon the cutting tools employed. The Sb-doped content in each semiconductor has been compared with the associated quantities such as the concentration and the conductivity range given by the sample donor. Uncertainty in the sodium analysis due to the fission neutron reaction by silicon itself was discussed.

Introduction

Trace impurities are believed to play a significant role in determining the mechanical and electrical properties of semiconductor silicon. However, in the majority of cases it is not possible to estimate theoretically the effects of different impurities on these properties. For this reason, ideally the semiconductor silicon should be free of all of the elements so as to meet requirements of "absolute purity" placed on the silicon.[1,2] Such requirements need survey analysis methods, which enable a maximum number of impurities or some of the dopant components to be determined. In addition, the purity of ultra pure semiconductors as well as the contents of some dopants are further checked by electrophysical methods which offer a means of estimating performance characteristics.

Silicon semiconductors which meet requirements of "absolute purity" would be ideal samples for instrumental neutron activation analysis (INAA). The matrix has a small activation cross-section, enabling analysis of silicon to be performed for 40-45[1,3] elements. The ideality of INAA for ultra pure silicon remains valid even for the analysis of some dopant components.

The purpose of the present work was to estimate the possibility of using INAA for the survey analysis of ultratrace impurities and some dopants in semiconductor grade silicon crystals of different origins. An attempt has also been made to determine some differences of impurity contents between doped and undoped silicon samples due to possible contamination during the doping processes. The extrinsic conductivity of Sb-doped semiconductors has been estimated by analytical data and compared with that obtained by the electrophysical method.

In the present investigation, nondestructive neutron activation analysis was carried out by the single comparator method with a Ge gammaray spectrometer as descrived previously[4,5]. The method is advantageous for the simultaneous determination of various elements in samples and its reliability is similar to that of the relative method[4,5].

Experimental

Apparatus. Gamma-counting was done with a Ge detector of 70cc volume coupled to a 4096 channel analyzer and a PDP-11 computer system. The system resolution was better than 1.9 KeV (FWHM at 1.33 MeV) with a peak-to-Compton ratio of 40:1. The data for the spectra were computed for the decay-corrected peak areas as described previously.[6]

Sample Preparation. The silicon samples analysed were either bulk or sliced. The bulk samples were cut to the weight of ca. 3g from a single-or polycrystal silicon rod. The slice samples were cut similarly from wafers. The bulk and slice samples were washed in a teflon beaker with trichloroethylene, acetone and deionized water, etched with a mixture of nitric and hydrochloric acid (1:3) and etched again with a mixture of nitric and hydrofluoric acid (10:1). The samples were then rinsed in deionized water and ethanol. The samples were weighed and sealed in a silica glass vial which had been treated similarly.

Neutron Activation Analysis. A known amount of Au